Optics & Laser Technology 154 (2022) 108303

Contents lists available at ScienceDirect

Optics and Laser Technology

journal homepage: www.elsevier.com/locate/optlastec

Full length article

Laser phase noise suppression and quadratures noise intercoupling in a mode cleaner

Nanjing Jiao [a], Ruixin Li [a], Yajun Wang [a,b,**], Wenhui Zhang [a], Chaoqun Zhang [a], Long Tian [a,b], Yaohui Zheng [a,b,*]

[a] State Key Laboratory of Quantum Optics and Quantum Optics Devices, Institute of Opto-Electronics, Shanxi University, Taiyuan 030006, China
[b] Collaborative Innovation Center of Extreme Optics, Shanxi University, Taiyuan, Shanxi 030006, China

ARTICLE INFO

Keywords:
Quadratures noise intercoupling
Mode cleaner
Phase noise characterization

ABSTRACT

Suppression phase noise of a laser is a great practical significance in applications of phase-sensitive precision measurement. To suppress the phase noise, an ultra-stable cavity incorporating with an electrical feedback control loop is always the popular choice, in which the linewidth of the cavity should be narrower than that of the laser to provide a stable reference standard. Here, we experimentally verify that mode cleaner plays a noise suppression role for phase quadrature in the whole frequency range of the photoelectric detectors, even though its linewidth is 10^3 larger than the laser one. Meanwhile, we found that the noise suppression for one quadrature is codetermined by the noise of the two quadratures of the input field. Our demonstration provides a new and in-depth interpretation for phase noise suppression in a mode cleaner with larger linewidth than the laser one that is important in phase-sensitive sensing application.

1. Introduction

Continuous wave (CW) single-frequency laser has been widely used in the field of quantum states preparation [1,2], optical clocks [3–5], gravitational wave detection [6,7] and so on, because of its advantages in narrow linewidth, low amplitude/phase noise and good stability. However, it operates not absolutely single-frequency, which is always accompanied by phase noise. The derivative of the phase to time is proportional to the instantaneous frequency, hence the phase noise will cause an instantaneous jitter of the laser beam in frequency domain. It is defined to evaluate the short-term stability, linewidth or coherent length of a laser. In squeezed state preparation, phase noise is equivalent to couple the anti-squeezed noise into the squeezed quadrature, which seriously decreases the squeezing level especially the noise reduction beyond 10 dB [2,8–14]. In gravitational wave detection, larger phase noise limits the sensitivity of the laser interferometer to a lower level by introducing a frequency noise in the cavity arm [15,16]. Furthermore, phase noise makes the frequency standard of the optical atomic clock unstable, thus decreasing its accuracy [5]. Therefore, it is of great practical significance to suppress the phase noise in applications [16–20].

Phase noise represents a random phase fluctuation of the laser with time, which results from the spontaneous emission of a lasing process [21]. To suppress the phase noise of a laser, an ultra-stable cavity with narrower linewidth and lower transmissivity incorporating with an electrical feedback control loop is always the popular choice [22,23]. But the bandwidth of feedback loop sets a limitation to phase noise suppression at kHz region. Optical filter cavity is widely applied for spectral and spatial cleaning of a laser beam, i.e., acting as a mode cleaner [24]. An optical feedback combining with a filter cavity method was proposed to suppress the diode laser phase noise in MHz frequency region, but careful optimizing of the feedback optical power should be carried out [25]. If not, the authors speculate that the phase noise maybe converts into amplitude one due to a dispersion optical character of the cavity, and is harmful in practical applications. However, the authors declared that no phase noise reduction of the optical filter was observed without the optical feedback control loop. A symmetric Fabry–Perot cavity was theoretically demonstrated as a low-pass filter for both amplitude and phase noise, and it also can be used to convert the phase noise into amplitude one [22]. Therefore, a second cavity is utilized to

* Corresponding author at: State Key Laboratory of Quantum Optics and Quantum Optics Devices, Institute of Opto-Electronics, Shanxi University, Taiyuan 030006, China.
** Principal corresponding author.
E-mail addresses: YJWangsxu@sxu.edu.cn (Y. Wang), yhzheng@sxu.edu.cn (Y. Zheng).

https://doi.org/10.1016/j.optlastec.2022.108303
Received 27 March 2022; Received in revised form 1 May 2022; Accepted 16 May 2022
Available online 26 May 2022

characterize the phase noise of a diode laser with near shot noise limited amplitude noise. However, the characterization method only limits the phase noise measurement at separated frequencies (1 MHz and 0.5 MHz), and the measurement is only valid under no excess amplitude noise. In these researches, the experimental demonstration of a phase noise suppression can not eliminate the effect of narrowing the laser linewidth with a high finesse cavity except for Ref. [25].

In this Letter, we suppress laser phase noise at RF region in virtue of a mode cleaner, verifying that the mode cleaner (MC) plays a noise suppression role for both amplitude and phase quadratures even though its linewidth is 10^3 larger than the laser one. Meanwhile, we also firstly demonstrate that the noise suppression for one quadrature is co-determined by the two quadratures of the input field more than a process of phase noise converting to an amplitude one. Further, a rotation of noise ellipse technique is applied to conveniently characterize the phase noise in a broadband noise spectrum and which results are in good agreement with the theoretical ones.

2. Experimental setup for phase noise suppression and characterization

Fig. 1 shows a simplified schematic of our experimental setup. The laser source is a continuous-wave single-frequency 1550 nm fiber laser with an output power of 30 mW and a linewidth of < 1 kHz (NKT, Koheras BASIK X15). Its output is divided into two parts by a beam splitter (BS), one is directly injected into the over-coupled cavity (OCC), and the remaining part is prepared for the input of a MC. A homemade electro-optic modulator (EOM) is used to generate a phase modulated signal of the 34.3 MHz for Pound-Drever-Hall locking of the MC. In this experiment, two MCs are alternated to act as the noise filter for both amplitude and phase quadratures of the laser. The reflectivity of the input and output mirrors of the MC1 is 99%, corresponding to a linewidth of 2.5 MHz, and that of the MC2 has a reflectivity of 90% with a linewidth of 35 MHz. Therefore, the MC is an impedance matched resonator, and nearly all the incident beam transmits from its output coupler with cavity on resonance. It can be regarded as a low-pass filter to suppress the high-frequency noise of the output field out of the linewidth. OCC is an over-coupled cavity, the reflectivity of the input coupler is 97%, and output one is better than 98.5%, corresponding to a linewidth of $\delta\nu_c$=7.5 MHz. The lengths of the three cavities are 426 mm. The incident light is nearly fully reflected from the cavity. With half-detuning, the reflected light field produces a phase shift of $\pi/2$, to convert the phase noise into an amplitude one. Two shutters are installed to control one of the two beams pour into the OCC.

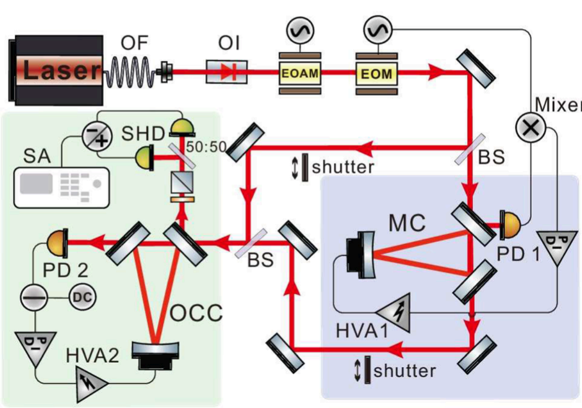

Fig. 1. Schematic overview of the experimental setup. OF, optical fiber; OI, optical isolator; MC, mode clear; BS, beam splitter; OCC, over-coupled cavity; 50:50, 50:50 beam splitter; SHD, self-homodyne detectors; EOM, electro-optic modulator; EOAM, electro-optic amplitude modulator; PD1,2, photodetector; SA, spectrum analyzer; PID, proportional-integral-derivative; HVA1,2, high-voltage amplifier.

A "rotation of the noise ellipse of light" technique is used to characterize the phase noise [22], which is equivalent to an inhomodyne detection without extra noise. The central theme is that an OCC with half linewidth detuning introduces a $\pi/2$ or $3\pi/2$ phase delay between the carrier and sidebands (the red curve in Fig. 2(a)). It makes the phase noise fully convert into an amplitude one due to a noise ellipse rotate to a orthogonal direction (Fig. 2(b)), which can be directly read out by a photoelectronic detector. In our experiment, an electro-optic amplitude modulator (EOAM) is used to impress pure amplitude modulated sidebands to the carrier, which is devoted to distinguish the amplitude quadrature from the phase one, and observe a full conversion of phase to amplitude noise. The transmitted beam of the OCC is applied to lock the OCC to an arbitrary detuning frequency, in which the DC output of PD2 is differentially amplified with an adjustable low noise DC voltage to generate an error signal. The reflected beam is poured into the self-homodyne detectors for amplitude quadrature measurement, and the addition or subtraction of the outputs of the two detectors are corresponding to the noise of amplitude quadrature noise and shot noise limited (SNL).

To ensure an efficient broadband noise spectrum measurement, we design a calibration method to checkout the phase noise characterization process in detail. Firstly, the optimum condition for full conversion of phase to amplitude noise is experimentally carried out. The laser beam is modulated with 37 MHz by the EOAM, which is far from the linewidth of the OCC to avoid a phase hopping during the characterization of the phase noise conversion. By directly guiding the laser beam into OCC, the conversion efficiency can be observed by the modulated amplitude peak noise power from the output of the self-homodyne detectors, i.e., it is similar with the peaks in Fig. 4. Thereupon, the conversion efficiency of phase to amplitude noise can be read out by the height of modulated amplitude peaks with an electrical spectrum analyzer (ESA), shown in Fig. 2(a). At the beginning, OCC operates at far detuning condition ($\nu = 3\delta\nu_c$, point ①in Fig. 2(a)). By continuous adjusting the DC voltage in the control loop of OCC, Δ is gradually changed from far detuning to half-linewidth detuning (point ③in Fig. 2 (a) corresponding to a phase shift of $\pi/2$). Under this circumstance, the modulated amplitude signal completely disappears from the noise spectrum of the reflected light of OCC, which indicates a full conversion of the phase to amplitude noise (Fig. 2(b) case ③). Further increasing the voltage value, the cavity reaches the resonance condition at point ⑤and the output beam is inverse phase with the input one. The measured noise power holds as the amplitude quadrature, and the coversion efficiency of the phase noise returns to zero (point or case ⑤in Fig. 2(a) or (b)). Next, higher voltage drives the cavity away from resonance, and shows up an inverse process as the above steps (⑤, ⑦, ⑨). Therefore, the optimum conditions for full conversion of phase to amplitude noise are experimentally confirmed, i.e., points ③and ⑦corresponding to the half-linewidth cavity detuning of the OCC. The noise ellipse rotation process in a phase space is also shown in Fig. 2(b), which is one-to-one correspondence to the points in Fig. 2(a). In the

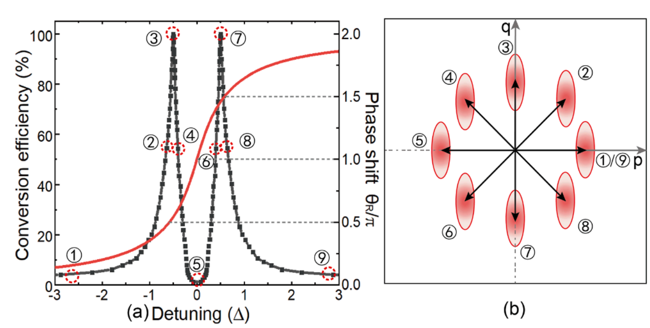

Fig. 2. (a) The relationship between conversion efficiency, phase shift and detuning parameter Δ, measured with the setup in Fig. 1. (b) Rotation of the noise ellipse in phase space evolving with the carrier detuning in one cycle.

experiment, the length detuning is completed by adjusting the high voltage applied to the PZT adhered on the concave mirror of the OCC. Firstly, the cavity is locked to resonance with a certain voltage. Then, a higher voltage will drive the length stretching to produce a negative detuning, otherwise a lower voltage produces a positive detuning.

Subsequently, the OCC is steadily locked to half-linewidth detuning for converting the phase noise to amplitude one. When the modulation frequency of the EOAM is continuously changed from 5 to 50 MHz, and the peak of the modulated amplitude constantly decreases until it gets to zero. We proved that, only when the modulated frequency of the EOAM is higher than 11 MHz, the modulated amplitude peak disappears. This approximately corresponds to $\sqrt{2}$ times of the OCC linewidth, which is consistent with the theoretical prediction in Ref. [26]. Hence, the rotation of the noise ellipse for $\pi/2$ phase shift maintains as the analysis frequency more than $\sqrt{2}$ times of the OCC linewidth, and within this frequency the noise ellipse rotation presents a frequency dependent characteristic.

3. Theoretical model and analysis for quadratures noise suppression and intercoupling

In this section, we begin to introduce the numerical method for phase noise analysis of a symmetric cavity with the model proposed in Ref. [26]. For phase noise at frequency ν of a given laser field, the power spectral density can be derived from the Wiener-Khinchin theorem for an ergodic process as [26,22]:

$$(q)_\nu^2 = \frac{1}{2\pi}\int d\nu' \langle \delta q(\nu)\delta q(\nu')\rangle \tag{1}$$

where $\pm\nu$ is the analysis frequency of the sidebands (beating with the carrier) symmetrically located around the carrier. For a coherent state $(q)_\nu^2 = 1/4$. And Eq. (1) is also valid for the amplitude quadrature $(p)_\nu^2$. The noise transfer characteristics of the amplitude and phase quadrature can be described by the input–output relations of the MC,

$$\begin{aligned}\begin{bmatrix}\delta p_{out}(\nu)\\ \delta q_{out}(\nu)\end{bmatrix} &= \begin{bmatrix}T_1(\Delta_0,\nu) & T_2(\Delta_0,\nu)\\ -T_2(\Delta_0,\nu) & T_1(\Delta_0,\nu)\end{bmatrix}\begin{bmatrix}\delta p_{in}(\nu)\\ \delta q_{in}(\nu)\end{bmatrix}\\ &+\begin{bmatrix}R_1(\Delta_0,\nu) & R_2(\Delta_0,\nu)\\ -R_2(\Delta_0,\nu) & R_1(\Delta_0,\nu)\end{bmatrix}\begin{bmatrix}\delta p_\mu(\nu)\\ \delta q_\mu(\nu)\end{bmatrix}\\ &+\sqrt{1-T_0}\begin{bmatrix}\delta p_w(\nu)\\ \delta q_w(\nu)\end{bmatrix}\end{aligned} \tag{2}$$

where Δ_0 is the detuned frequency of the carrier ν_0 from the cavity resonance, μ represents the vacuum field entering from the output coupler, ω is the vacuum field introduced by the loss channels of the MC, and T_0 is transmissivity on resonance of the cavity. $\delta p_\mu, \delta q_\mu, \delta p_\omega$ and δq_ω are the quadrature phase and amplitude operators for two vacuum fields, and the elements of the matrix are defined as:

$$\begin{aligned}T_1(\Delta_0,\nu) &= [T(\Delta_0+\nu)+T(\Delta_0-\nu)^*]/2,\\ T_2(\Delta_0,\nu) &= i[T(\Delta_0+\nu)-T(\Delta_0-\nu)^*]/2,\\ R_1(\Delta_0,\nu) &= [R(\Delta_0+\nu)+R(\Delta_0-\nu)^*]/2,\\ R_2(\Delta_0,\nu) &= i[R(\Delta_0+\nu)-R(\Delta_0-\nu)^*]/2.\end{aligned} \tag{3}$$

where the transmission and reflection coefficients for the MC are given by:

$$\begin{aligned}T(\Delta) &= \frac{\sqrt{T_0}}{1-i2\Delta/\Gamma},\\ R(\Delta) &= \frac{-i\sqrt{T_0}2\Delta/\Gamma}{1-i2\Delta/\Gamma}.\end{aligned} \tag{4}$$

here defines a detuning parameter $\Delta = \nu/\delta\nu_c$. Γ is the FWHM linewidth.

For a given input optical field and a cavity with a linewidth of 10^3 larger than the laser one, three cases of input quadrature noise are considered to analysis the output power spectral density, quantitatively calculated by Eqs. (1) to (4) with the experimental parameters in our configuration. The input–output relations of the quadrature noises are shown in Fig. 3, (a) the amplitude noise and phase noise of the input field are both 20 dB, and (b) the amplitude noise is 0 dB and phase noise is 20 dB, or the amplitude noise is 20 dB and phase noise is 0 dB (It is omitted to avoid of repetition.). The theoretical results indicate that MC has a low-pass filtering property for both amplitude and phase noises, and each quadrature noise is codetermined by that of both quadratures of the input field. It means that the two quadrature noises of the input field are intercoupled with each other by the MC, due to a detuning induced phase shift of the sidebands. Therefore, if the amplitude noise of the input field is lower than the phase one or meets the shot noise limited level, the output amplitude noise shows a remarkable rising trend due to a larger contribution of the input phase noise.

4. Experimental results and analysis of quadratures noise suppression

In our experiment, the phase noises before and after MC are characterized with the "rotation of noise ellipse of light" technique. While the amplitude noise comparation is calibrated by far detuning of the OCC. To distinguish the two quadratures, a 16 MHz sideband signal is amplitude modulated by the EOAM to the upstream laser of the MC.

The measured amplitude and phase noise powers of the two quadratures are shown in Fig. 4 and Fig. 5, corresponding to the outputs of MCs with linewidths of 35 MHz and 2.5 MHz, respectively. The data is recorded with a laser power of 1.38 mW for each of the self-homodyne detectors. The results confirm that MC has a noise filter speciality in a broadband noise spectrum for both amplitude and phase noises despite the cavity linewidth is 10^3 larger than the laser linewidth (kHz), which is different from most of the already published experimental literatures, only focusing on the amplitude noise suppression [27] or phase noise suppression for narrowing the laser linewidth with high finesse optical cavity [8,9,28–30]. Meanwhile, Fig. 5 also proves that narrower linewidth MC could suppress both amplitude and phase noises to SNL at lower analysis frequency, meanwhile it reduces larger excess quadrature noise than the larger linewidth MC in the frequency range of 5–50 MHz, especially beyond its linewidth. In illustration of Fig. 4(b) and Fig. 5(b), the modulated amplitude peak (16 MHz) is suppressed to the amplitude noise floor, due to a far detuning frequency compared with the linewidth of the MC (2.5 MHz). Here, we fit the experimental results with theoretical Eqs. (1)–(4), in which all the spectral density of the amplitude and phase noise are in good agreement with the theoretical results (dashed lines of FPN1 and FAN1). It further verifies the efficient of a broadband phase noise measurement with "rotation of the noise ellipse of light" technique. To analyze the constituent ratio of the noise source of the output field, the other two theoretical curves FAN2 and FPN2 are presented in Fig. 4. FAN2 or FPN2 is independently calculated only with the phase noise or amplitude noise of the input filed. In comparison with the fitted curves of FPN1 and FAN1, FPN2 and FAN2 have large deviations from the experimental data, which demonstrate a noise

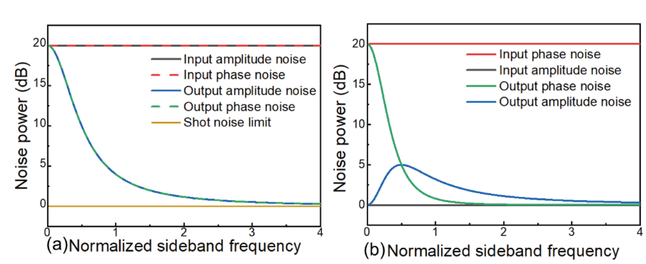

Fig. 3. Theoretical noise transmission of a mode cleaner for the amplitude (a) and phase (b) noise reduction.

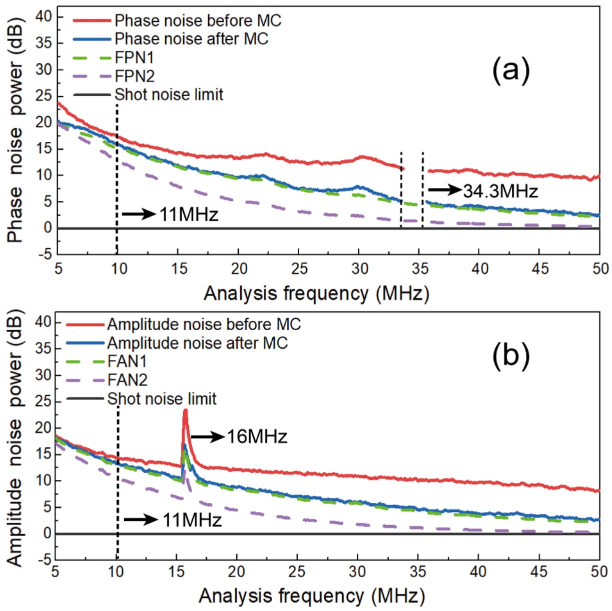

Fig. 4. Laser noise characteristic versus analysis frequency with a MC linewidth of 35 MHz. (a) Phase noise before and after MC. (b) Amplitude noise before and after MC. The black line is the normalized shot noise limit, the red line is the phase/amplitude noise of the beam before MC, and the blue line is that of after MC, the green/purple line is the fitted one after MC. FPN1, 2: fitted phase noise with two quadratures noise (1) or only with phase noise (2); FAN1, 2: fitted amplitude noise with two quadratures noise (1) or only with amplitude noise (2). (For interpretation of the references to colour in this figure legend, the reader is referred to the web version of this article.)

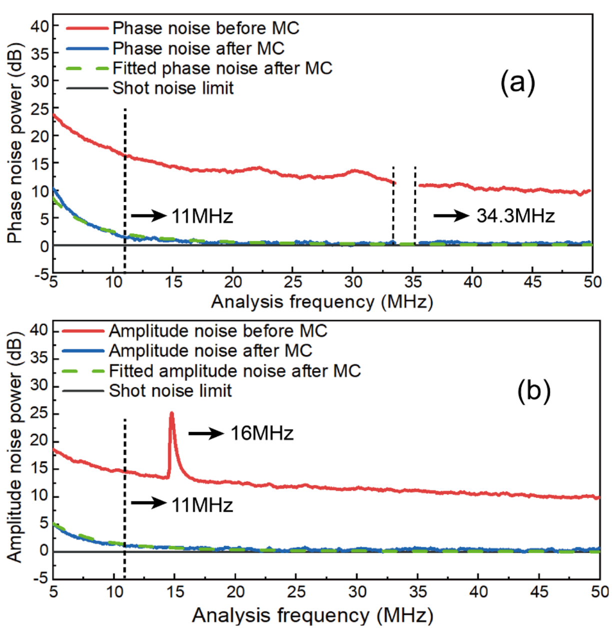

Fig. 5. Laser noise characteristic versus analysis frequency with a MC linewidth of 2.5 MHz. (a) Phase noise before and after MC. (b) Amplitude noise before and after MC. The black line is the normalized shot noise limit, the red line is the phase/amplitude noise of the beam before MC, and the blue line is that of after MC, the green line is the fitted one after MC. (For interpretation of the references to colour in this figure legend, the reader is referred to the web version of this article.)

intercoupling between the amplitude quadrature and phase one existing in the transmission of MC. Different from the claim for phase noise converting to amplitude one[22,25], we found that the two quadrature noises of the input field codetermine the output noise power for one quadrature.

5. Conclusion

We have experimentally demonstrated a phase noise suppression scheme at RF region in virtue of an optical mode cleaner with a linewidth of 10^3 larger than the laser one for broadband noise spectrum. The phase and amplitude noise before and after the optical mode cleaner are directly measured with a noise ellipse rotation technique, and the results indicate that the noise reduction is accomplished by a noise intercoupling between the two quadratures. The results are in good agreement with the theoretical ones. Our proposal provides a solution and interpretation for direct phase characterization and suppression with a simple scheme.

Funding

National Key Research and Development Program of China (2020YFC2200402); National Natural Science Foundation of China (NSFC) (62027821, 11874250, 62035015, 12174234); Key Research and Development Projects of Shanxi Province (202102150101003, 201903D111001); Program for Sanjin Scholar of Shanxi Province.

Declaration of Competing Interest

The authors declare that they have no known competing financial interests or personal relationships that could have appeared to influence the work reported in this paper.

References

[1] M. Mehmet, H. Vahlbruch, High-efficiency squeezed light generation for gravitational wave detectors, Class. Quant. Grav. 36 (1) (2018) 015014.
[2] E. Oelker, G. Mansell, M. Tse, J. Miller, F. Matichard, L. Barsotti, P. Fritschel, D. McClelland, M. Evans, N. Mavalvala, Ultra-low phase noise squeezed vacuum source for gravitational wave detectors, Optica 3 (7) (2016) 682–685.
[3] R. Le Targat, L. Lorini, Y. Le Coq, M. Zawada, J. Guéna, M. Abgrall, M. Gurov, P. Rosenbusch, D. Rovera, B. Nagórny, et al., Experimental realization of an optical second with strontium lattice clocks, Nat. Commun. 4 (1) (2013) 1–9.
[4] M. Schulte, C. Lisdat, P.O. Schmidt, U. Sterr, K. Hammerer, Prospects and challenges for squeezing-enhanced optical atomic clocks, Nat. Commun. 11 (1) (2020) 1–10.
[5] B.A.C.O.N.B. Collaboration, Frequency ratio measurements at 18-digit accuracy using an optical clock network, Nature 591 (7851) (2021) 564–569.
[6] M. Steinke, H. Tünnermann, V. Kuhn, T. Theeg, M. Karow, O. de Varona, P. Jahn, P. Booker, J. Neumann, P. Weßels, et al., Single-frequency fiber amplifiers for next-generation gravitational wave detectors, IEEE J. Sel. Top. Quantum Electron. 24 (3) (2017) 1–13.
[7] F. Wellmann, M. Steinke, F. Meylahn, N. Bode, B. Willke, L. Overmeyer, J. Neumann, D. Kracht, High power, single-frequency, monolithic fiber amplifier for the next generation of gravitational wave detectors, Opt. Express 27 (20) (2019) 28523–28533.
[8] H. Vahlbruch, M. Mehmet, K. Danzmann, R. Schnabel, Detection of 15 db squeezed states of light and their application for the absolute calibration of photoelectric quantum efficiency, Phys. Rev. Lett. 117 (11) (2016) 110801.
[9] W. Yang, S. Shi, Y. Wang, W. Ma, Y. Zheng, K. Peng, Detection of stably bright squeezed light with the quantum noise reduction of 12.6 db by mutually compensating the phase fluctuations, Opt. Lett. 42 (21) (2017) 4553–4556.
[10] W. Zhang, J. Wang, Y. Zheng, Y. Wang, K. Peng, Optimization of the squeezing factor by temperature-dependent phase shift compensation in a doubly resonant optical parametric oscillator, Appl. Phys. Lett. 115 (17) (2019) 171103.
[11] W. Zhang, N. Jiao, R. Li, L. Tian, Y. Wang, Y. Zheng, Precise control of squeezing angle to generate 11 db entangled state, Opt. Express 29 (15) (2021) 24315–24325.
[12] L. Tian, S. Shi, Y. Li, Y. Wu, W. Li, Y. Wang, Q. Liu, Y. Zheng, Entangled sideband control scheme via frequency-comb-type seed beam, Opt. Lett. 46 (16) (2021) 3989–3992.
[13] S. Shi, L. Tian, Y. Wang, Y. Zheng, C. Xie, K. Peng, Demonstration of channel multiplexing quantum communication exploiting entangled sideband modes, Phys. Rev. Lett. 125 (7) (2020) 070502.
[14] Y. Han, X. Wen, J. Liu, J. He, J. Wang, Generation of polarization squeezed light with an optical parametric amplifier at 795 nm, Optics Communications 416 (2018) 1–4.
[15] M. Pitkin, S. Reid, S. Rowan, J. Hough, Gravitational wave detection by interferometry (ground and space), Living Rev. Relativ. 14 (1) (2011) 1–75.

[16] C. Cahillane, G.L. Mansell, D. Sigg, Laser frequency noise in next generation gravitational-wave detectors, Opt. Express 29 (25) (2021) 42144–42161.
[17] X. Sun, Y. Wang, L. Tian, S. Shi, Y. Zheng, K. Peng, Dependence of the squeezing and anti-squeezing factors of bright squeezed light on the seed beam power and pump beam noise, Opt. Lett. 44 (7) (2019) 1789–1792.
[18] X. Sun, Y. Wang, Y. Tian, Q. Wang, L. Tian, Y. Zheng, K. Peng, Deterministic and universal quantum squeezing gate with a teleportation-like protocol, Laser & Photonics Reviews (2021) 2100329.
[19] Q. Wang, Y. Wang, X. Sun, Y. Tian, W. Li, L. Tian, X. Yu, J. Zhang, Y. Zheng, Controllable continuous variable quantum state distributor, Opt. Lett. 46 (8) (2021) 1844–1847.
[20] Z. Ren, K. Cui, J. Li, R. Zhu, W. Peng, J. Qian, A high-quality phase modulation scheme with strong noise-suppressing capability for interferometric fiber-optic sensor applications, Opt. Lasers Eng. 118 (2019) 34–41.
[21] V. Lovic, D.G. Marangon, M. Lucamarini, Z. Yuan, A.J. Shields, Characterizing phase noise in a gain-switched laser diode for quantum random-number generation, Phys. Rev. Appl. 16 (5) (2021) 054012.
[22] J. Hald, V. Ruseva, Efficient suppression of diode-laser phase noise by optical filtering, JOSA B 22 (11) (2005) 2338–2344.
[23] C. Cahillane, G.L. Mansell, D. Sigg, Laser frequency noise in next generation gravitational-wave detectors, Opt. Express 29 (25) (2021) 42144–42161.
[24] B. Willke, N. Uehara, E. Gustafson, R. Byer, P. King, S. Seel, R. Savage, Spatial and temporal filtering of a 10-w nd: Yag laser with a fabry–perot ring-cavity premode cleaner, Opt. Lett. 23 (21) (1998) 1704–1706.
[25] Y. Zhang, S. Miyakawa, K. Kasai, Y. Okada-Shudo, M. Watanabe, Efficient phase noise suppression of an external-cavity diode-laser by optical filtering and resonant optical feedback, Appl. Phys. B 108 (1) (2012) 39–42.
[26] A.S. Villar, The conversion of phase to amplitude fluctuations of a light beam by an optical cavity, Am. J. Phys. 76 (10) (2008) 922–929.
[27] X. Sun, Y. Wang, L. Tian, Y. Zheng, K. Peng, Detection of 13.8 db squeezed vacuum states by optimizing the interference efficiency and gain of balanced homodyne detection, Chinese Optics Letters 17 (7) (2019) 072701.
[28] O. Llopis, P.-H. Merrer, H. Brahimi, K. Saleh, P. Lacroix, Phase noise measurement of a narrow linewidth cw laser using delay line approaches, Opt. Lett. 36 (14) (2011) 2713–2715.
[29] N. Huntemann, C. Sanner, B. Lipphardt, C. Tamm, E. Peik, Single-ion atomic clock with 3×10^{-18} systematic uncertainty, Phys. Rev. Lett. 116 (6) (2016) 063001.
[30] B. Bloom, T. Nicholson, J. Williams, S. Campbell, M. Bishof, X. Zhang, W. Zhang, S. Bromley, J. Ye, An optical lattice clock with accuracy and stability at the 10^{-18} level, Nature 506 (7486) (2014) 71–75.